

# Wireless power transfer in attenuating media

Cite as: AIP Advances **11**, 115303 (2021); <https://doi.org/10.1063/5.0059932>

Submitted: 14 June 2021 • Accepted: 06 October 2021 • Published Online: 01 November 2021

 S. Chu, C. J. Stevens and E. Shamonina

## COLLECTIONS

Paper published as part of the special topic on [Biophysics and Bioengineering](#)



View Online



Export Citation



CrossMark

## ARTICLES YOU MAY BE INTERESTED IN

[A 3D passive micromixer with particle of stochastic motion through limonene dissolution method](#)

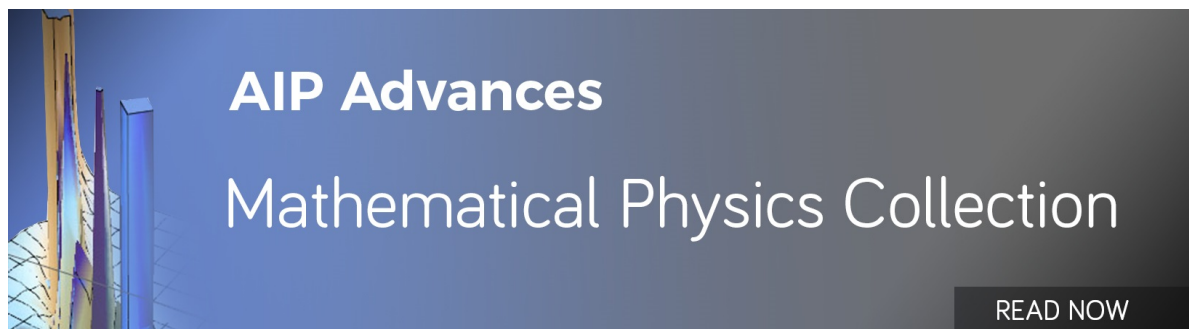
AIP Advances **11**, 105318 (2021); <https://doi.org/10.1063/5.0067135>

[Roadmap on organic–inorganic hybrid perovskite semiconductors and devices](#)

APL Materials **9**, 109202 (2021); <https://doi.org/10.1063/5.0047616>

[Hydrogel: A potential therapeutic material for bone tissue engineering](#)

AIP Advances **11**, 010701 (2021); <https://doi.org/10.1063/5.0035504>



# Wireless power transfer in attenuating media

Cite as: AIP Advances 11, 115303 (2021); doi: 10.1063/5.0059932

Submitted: 14 June 2021 • Accepted: 6 October 2021 •

Published Online: 1 November 2021



S. Chu,<sup>1,a)</sup>  C. J. Stevens,<sup>2</sup> and E. Shamonina<sup>2</sup>

## AFFILIATIONS

<sup>1</sup>Institute of Neuroscience and Psychology, University of Glasgow, Glasgow G51 4TF, United Kingdom

<sup>2</sup>Department of Engineering Science, University of Oxford, Oxford OX1 3PJ, United Kingdom

<sup>a)</sup>Author to whom correspondence should be addressed: [son.congchu@glasgow.ac.uk](mailto:son.congchu@glasgow.ac.uk)

## ABSTRACT

Dissipative media (underground/underwater, biological materials and tissues, etc.) pose a challenge to inductive wireless power transfer systems as they generally attenuate the near fields that enable mutual coupling. Apart from this, the impact of the environment on electromagnetic fields can also be seen in the self-impedance of coils, resulting in significant eddy current losses and detuning effects. In this article, we study, theoretically, the mechanism of wireless power transfer via a pair of magnetic resonators inside an infinite homogeneous medium with a comprehensive circuit model that takes into account all the electromagnetic effects of the background medium. This analytical approach can offer deep insights into the design and operation of wireless charging systems in non-ideal environments.

© 2021 Author(s). All article content, except where otherwise noted, is licensed under a Creative Commons Attribution (CC BY) license (<http://creativecommons.org/licenses/by/4.0/>). <https://doi.org/10.1063/5.0059932>

Wireless power transfer (WPT) via strongly coupled magnetic resonators is a subject of much recent interest, with significant competition between standards and approaches.<sup>1–4</sup> To date, transferring power to sensors in underground/underwater systems or *in vivo* medical devices has attracted increasing attention due to their short battery lifetime.<sup>5</sup> Among various methods for wireless power and data transmission for implantable biomedical devices (acoustic power transfer, optical methods, capacitive coupling, and intra-body communication), near-field magnetic coupling is considered the most suitable approach since it can efficiently deliver power and information without harmful impact to living tissues. More details about the limitations of other methods can be found in Ref. 5. Unlike in the air or other lossless media, eddy currents are excited inside an attenuating transmission environment due to a time-varying magnetic field, according to Faraday's law of induction. As a result, they have a significant impact on the magnetic channels between two coupled resonators. Recent studies have shown that a dissipative medium generally has two major effects on the magnetic field produced by a loop current. First, the total magnetic field becomes elliptical because of the secondary magnetic field produced by the excited eddy currents, and second, the medium causes a phase shift in the magnetic field, which results in a complex mutual inductance.<sup>6,7</sup> Details of the parametric study on the effects of the transmission medium on the self- and mutual impedance of two coupled coils can be found in Refs 6–9.

With the inclusion of excited eddy currents, the mechanism for WPT in a dissipative medium is modified significantly compared to that in free space. Recent studies have paid significant attention to the impact of eddy currents on magnetically coupled resonators, such as complex mutual inductance,<sup>6,7,10–12</sup> eddy current loss,<sup>6,10–12</sup> and detuning effects.<sup>6,11,12</sup> However, from the theoretical point of view, the models used in these works seem to be incomplete. In Ref. 10, the detuning effects are excluded by neglecting the change in the self-inductance of the coils. This approximation may be adequate at low frequencies (typically kHz) but can be costly when the working frequency moves to MHz or higher. Advanced studies<sup>11,12</sup> have taken into account the eddy current loss and the detuning effects. Although these works proposed an analytical method to quantitatively evaluate the effects of eddy currents, some important parameters were obtained through simulation and experimental means.<sup>11,12</sup> Recently, the authors of Ref. 13 proposed an equivalent circuit model for two coupled resonators inside an arbitrary medium that analytically incorporates all electromagnetic couplings and feedback effects. By testing the dispersion relation of magnetoinductive waves in a dissipative medium, the equivalent circuit model is obliquely corroborated.<sup>13</sup> In this paper, with the circuit model proposed in Ref. 13, we elaborate the theory of WPT via a pair of coupled magnetic resonators inside an infinite homogeneous non-ideal environment.

The simplest configuration for WPT in dissipative media consists of two magnetically coupled coils insulated by dielectric cavities

and completely embedded in an infinite homogeneous medium, as shown in Fig. 1(a). Efficiency is improved by making these coils resonant. In general, dielectric cavities providing coil insulation are often made of common low-loss and low-permittivity polymers for hard-packaging, such as polyethylene (PE), polypropylene (PP), and polyvinyl chloride (PVC). As a result, they have little-to-no effect on the magnetic channels and hence are assumed to be free space. However, the dielectric cavities must be taken into account in the theoretical model when they are made of high-permittivity or high-loss materials [for example, the  $\text{Bi}_2(\text{Li}_{0.5}\text{Ta}_{1.5})\text{O}_7 + x\text{Bi}_2\text{O}_3$  ( $x = 0, 0.01$  and  $0.02$ ) ceramic has a relative permittivity of around  $60\text{--}70$ <sup>14</sup>].

The intrinsic capacitance of magnetic resonators is typically small, so to realize WPT at lower frequencies, additional tuning capacitors are required to form resonant tanks in both primary and secondary sides.<sup>3</sup> Concerning the capacitive tuning circuits, there are four possible simple topologies, namely, parallel-parallel, parallel-series, series-series, and series-parallel, standing for the connection type of the capacitors in the transmitting and receiving coils.<sup>4</sup> Some advanced compensation networks consisting of both inductors and capacitors, for example, the LLC network, can be found in Ref. 15. Here, within the scope of this paper, series-series topology is assumed because the value of external capacitors is independent of the magnetic coupling coefficient,<sup>4</sup> which varies significantly with respect to the medium properties.<sup>7,13</sup> No other external circuitry such as rectifiers, inverters, and regulators is considered in this work. Inside the medium, because of the impact of excited eddy currents, two of the terms in each circuit's Kirchhoff equation become complex—both self- and mutual inductance gain lossy components.<sup>6,13</sup> In the following, we refer the difference between the self-inductance of the coils in a lossy medium and that in free space as

“complex self-inductance,” which is a complex quantity. The imaginary part of complex self-inductance is associated with the power loss to the attenuating medium. While it may be roughly understood that the resistance of the resonators increases (or a lower Q-factor) due to the impact of the excited eddy currents, we emphasize that it is indeed the inductance, which is calculated by integrating the magnetic vector potential generated by the eddy currents over the volume of the coil itself.<sup>13</sup> As a result, unlike the resistance, it has a  $j\omega$ -frequency-dependence.

Using Kirchhoff's voltage law, the resulting equivalent circuit model for a WPT system in an attenuating medium, illustrated in Fig. 1(b), can be written as

$$\begin{bmatrix} R_s + Z_1 + j\omega\mathcal{L}_1 & j\omega\mathcal{M} \\ j\omega\mathcal{M} & Z_2 + j\omega\mathcal{L}_2 + R_L \end{bmatrix} \begin{bmatrix} I_1 \\ I_2 \end{bmatrix} = \begin{bmatrix} V_s \\ 0 \end{bmatrix}, \quad (1)$$

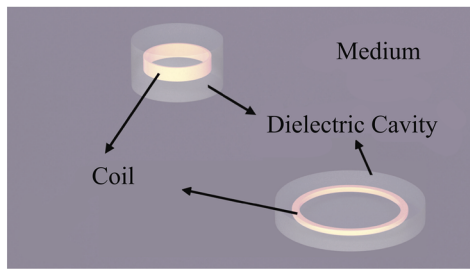
where  $\omega = 2\pi f$  is the angular frequency;  $V_s$  and  $R_s$  are the voltage and internal resistance of the source, respectively;  $R_L$  is the resistance of the load;  $I_i$ ,  $Z_i = R_i + j\omega L_i + 1/(j\omega C_i)$ ,  $R_i$ ,  $L_i$ , and  $C_i$  are the current response, impedance, resistance, self-inductance, and value of tuning capacitors of the coil  $i$ , respectively;  $\mathcal{L}_i$  is the complex self-inductance of coil  $i$ , representing the extra self-inductance and resistance it generates because of the eddy currents;  $\mathcal{M} = M_0 + M_E$  is the complex mutual inductance between two coils inside the medium;  $M_0$  is the mutual inductance of two coils in free space (typically a real number); and  $M_E$  represents the extra mutual coupling between the coils due to the eddy currents generated in the environment. In free space, eddy currents do not exist, and hence, all the additional couplings are zero, i.e.,  $\mathcal{L}_i = 0$ ,  $M_E = 0$ , and  $\mathcal{M} = M_0$ . The complex Kirchhoff coefficients are generally complex, i.e.,  $\mathcal{M} = \mathcal{M}' + j\mathcal{M}''$  and  $\mathcal{L}_i = \mathcal{L}_i' - j\mathcal{L}_i''$  (where  $-\mathcal{L}_i'' < 0$  because it is associated with the power loss in the medium<sup>13</sup>). Recalling that  $Z_i + j\omega\mathcal{L}_i = \tilde{R}_i + j\tilde{X}_i$ , where  $\tilde{R}_i = R_i + \omega\mathcal{L}_i''$ ,  $\tilde{X}_i = \omega L_i - 1/(\omega C_i)$  and  $\tilde{X}_i = X_i + \omega\mathcal{L}_i'$ , the output power at the load can then be calculated as

$$\begin{aligned} P_L &= \Re\{V_L I_L^*\} = |I_2|^2 R_L \\ &= \frac{\omega^2 |\mathcal{M}|^2 V_s^2 R_L}{|(R_s + Z_1 + j\omega\mathcal{L}_1)(Z_2 + j\omega\mathcal{L}_2 + R_L) + \omega^2 \mathcal{M}^2|^2} \\ &= \frac{\omega^2 (\mathcal{M}'^2 + \mathcal{M}''^2) V_s^2 R_L}{[(\tilde{R}_1 + R_s)(\tilde{R}_2 + R_L) + \omega^2 (\mathcal{M}'^2 - \mathcal{M}''^2) \tilde{X}_1 \tilde{X}_2]^2 + [2\omega^2 \mathcal{M}' \mathcal{M}'' + (\tilde{R}_2 + R_L) \tilde{X}_1 + (\tilde{R}_1 + R_s) \tilde{X}_2]^2}. \end{aligned} \quad (2)$$

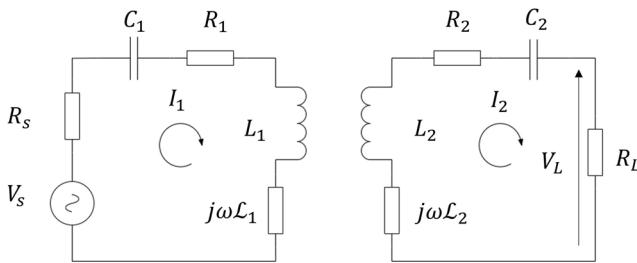
Unlike the free space case, the dissipative medium absorbs some of the power due to eddy current losses. The efficiency of the WPT in a conductive medium is written as

$$\eta = \frac{P_L}{P_{in}} = \frac{|I_2|^2 R_L}{\Re\{V_s I_1^*\}}. \quad (3)$$

In this paper, the optimal load expression is not derived at the resonant frequency as in most literature studies; instead, it is derived at an arbitrary frequency when the resonators have reactive impedance. The working frequency for the WPT systems in dissipative media is



(a)



(b)

**FIG. 1.** (a) and (b) Equivalent circuit model of a WPT system consisting of two resonant coils with series-series capacitive compensation topology.

then a parameter to be optimized. It is noted that conjugate matching, when a complex input impedance is present, is not considered because the paper aims to draw attention to the limitations of the current model when applied to systems in conductive media. Based

on (2), the output power may be maximized by adjusting the load resistance. Mathematically, the optimal load can be found by finding the roots of the first order derivative of (2) with respect to  $R_L$ , i.e.,  $dP_L/dR_L = 0$ ,

$$R_L = \sqrt{\frac{\omega^4 (\mathcal{M}'^2 + \mathcal{M}''^2)^2 + 2\omega^2 \{ (\mathcal{M}'^2 - \mathcal{M}''^2) (\tilde{R}_1 \tilde{R}_2 + \tilde{R}_2 R_s - \tilde{X}_1 \tilde{X}_2) + 2\mathcal{M}' \mathcal{M}'' [\tilde{R}_2 \tilde{X}_1 + (\tilde{R}_1 + R_s) \tilde{X}_2] \} + [(\tilde{R}_1 + R_s)^2 + \tilde{X}_1^2] (\tilde{R}_2^2 + \tilde{X}_2^2)}{(\tilde{R}_1 + R_s)^2 + \tilde{X}_1^2}}. \quad (4)$$

When the coupling is fixed, the maximum output power can be achieved with both primary and secondary circuits tuned to the same resonant frequency by adding suitable external capacitors to the windings, i.e.,  $f_{i0} = 1/(2\pi\sqrt{L_i C_i})$ , given the load is optimal and the loss in the windings is negligible.<sup>1</sup> However, as discussed in Ref. 13, the resonance frequency is shifted due to the effects of the eddy currents on self-inductance. Inside the medium, the resonant frequency  $f_{i0}$  of the coil  $i$  consequently shifts to  $\tilde{f}_{i0}$ . Since the complex Kirchhoff coefficients are frequency-dependent,  $\tilde{f}_{i0}$  is the root of the following equation representing the total reactance equaling to zero:

$$\tilde{f}_{i0}^2 (L_i - L'_i) - 1/(4\pi^2 C_i) = 0. \quad (5)$$

We note that the self-resonance of the coils varies with respect to the electromagnetic properties of the transmission medium. When the medium is highly permittive but weakly conductive, the self-resonance inside the medium is lower due to the flux reinforcement of the displacement eddy currents, making the total self-inductance higher.<sup>8,13</sup> As the conductivity increases, the conduction eddy currents induce an opposite EMF back to the transmitter, as expected from Lenz's law, so that the total self-flux reduces, shifting the resonance to higher frequencies.<sup>8,13</sup> As a result, the optimal working frequency for these systems may not be the original resonance of the windings in free space ( $f_0$ ). To deal with this problem, when considering a WPT system with a pair of coupled resonators above a conducting slab, authors in Ref. 6 suggested retuning the coil that is closest to the slab, which is strongly affected by the eddy currents, to the original resonant frequency by altering the external capacitors. Simulation results show that the retuning technique has the merit of increasing the useful power at the load in their case.<sup>6</sup> However, in our case, since the two coils are submerged in a dissipative medium, the medium detunes the two coils equally. The original resonance may not be the most advantageous frequency for such WPT systems.

In this section, we consider a case study where the primary and secondary coils of the simulated WPT system are assumed to be identical and placed coaxially at a distance from each other. The operating frequency of the system is the ISM band at 6.78 MHz, following the Rezenze A4WP standard.<sup>16</sup> The resistance of the coil is assumed to be constant around the resonant frequency. The WPT system is embedded inside a non-ideal environment, with a variable conductivity of up to  $\sigma = 100$  S/m, which is the highest value of all earth or biological materials.<sup>17,18</sup> Finally, the geometric and circuit parameters are summarized in Table I. The radius of the

dielectric boxes is assumed to be three times larger than the coil radius in order to calculate the complex Kirchhoff coefficients using the method in Ref. 13. Figure 2 shows the calculated output power at the original resonance and the optimal frequency vs the medium conductivity. The optimal frequency and load resistance determined by the location of the maximum power are presented in Figs. 2(c) and 2(d). For the purpose of comparison, the retuning method in Ref. 6 is included. In the retuning method, the resonant frequency of the resonators is fixed by adding suitable additional capacitors to compensate the impact of the eddy currents via complex self-inductance.<sup>6</sup>

As shown in Fig. 2(a), the retuning method appears to be not favorable compared to the non-retuned case as the two curves almost coincide. In addition, in practice, capacitors are not ideal and often modeled as capacitance in series with resistance, called "Equivalent Series Resistance" (ESR).<sup>19</sup> Inserting additional capacitors may thus cause losses due to ESR, and hence, it can be disastrous for the overall performance of WPT systems. Remarkably, in both non-retuned and retuned cases, the output power is not maximum at the original resonance for some particular media. When the conductivity is small, the medium seems to have little-to-no effect on the output power as the optimal frequency is practically the original resonance [see Fig. 2(c)]. The optimal frequency for the maximum output power then exhibits

TABLE I. Parameter list of the case study.

Mean coil radius, $r_0$	60 (mm)
Wire diameter, $r_w$	0.6 (mm)
Coil height	12 (mm)
Number of turns, $N$	10
Distance between coils	60 (mm)
Dielectric insulator radius	180 (mm)
Dielectric insulator height	14 (mm)
Resonance frequency, $f_0$	6.78 (MHz)
Self-inductance, $L$	23.3464 ( $\mu$ H)
Parasitic resistance, $R$	0.6793 ( $\Omega$ )
Mutual inductance (free space), $M_0$	2.9907 ( $\mu$ H)
AC voltage source, $V_s$	10 (V)
Internal source resistance, $R_s$	5 ( $\Omega$ )
Medium relative permittivity, $\epsilon_r$	78
Medium relative permeability, $\mu_r$	1
Medium conductivity, $\sigma$	$1 \times 10^{-3} - 1 \times 10^2$ (S/m)

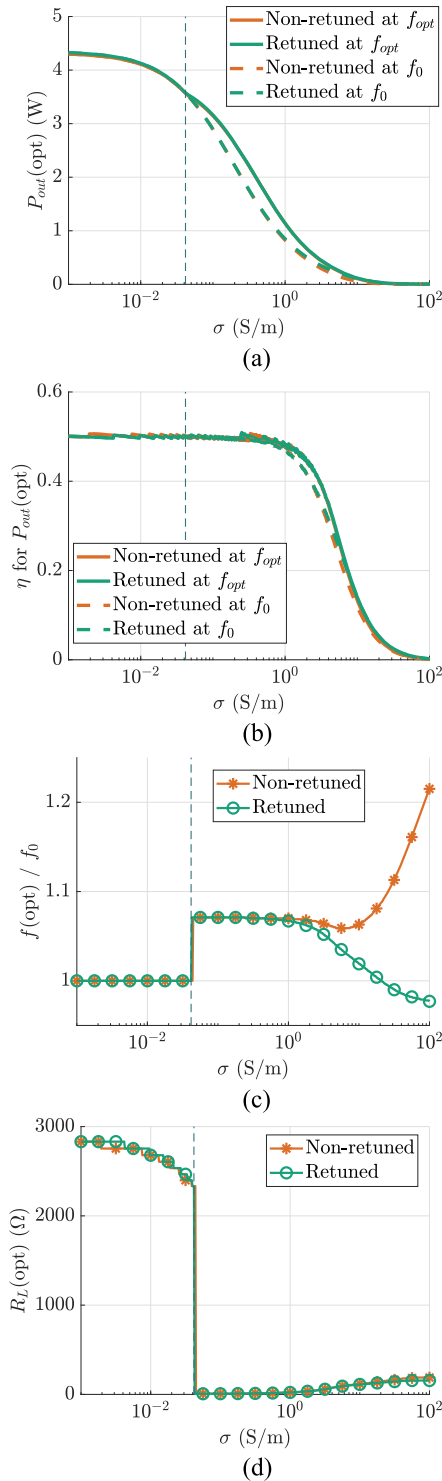


**FIG. 2.** (a) Calculated output power at load at the optimal frequency and the resonance, (b) the corresponding efficiency, (c) optimal frequency, and (d) optimal load resistance. In the retuned case, the compensation capacitances are added according to the prediction of the detuning effect, while in the non-retuned case, the compensation capacitances are kept the same as in free space.

a discontinuity jump to a higher frequency. This result is somewhat consistent with the experimental results presented in Ref. 20, where it is concluded that “the optimum operating frequency of a WPT system in seawater should be larger than the resonant frequency to achieve the maximum DC–DC efficiency.”

To examine the impact of medium conductivity on the discontinuity of the optimal frequency curve, Fig. 3 illustrates the 3D color plots of the output power vs the frequency and load resistance for four different conductivities:  $\sigma = 0.01, 1, 4$ , and  $10$  S/m. When the medium has a low conductivity, the output power always has its global maximum peaks at the resonant frequency, similar to the free-space case. When the load resistance is small, frequency splitting occurs as the output power exhibits two sharp peaks at the upper and lower resonances [see Figs. 3(a) and 3(b)]. In addition, as can be seen from the heights of the power peaks, the system undergoes different amounts of losses at variable frequency due to the frequency-dependent eddy currents. The power peaks at the lower resonance and the original resonance suffer from larger attenuation with increasing conductivity compared to the upper one. When the total losses are high enough, the lower resonance is completely suppressed while the peaks at the original resonance ( $f_0$ ) and upper resonance ( $f_u$ ) coalesce. In fact, the optimal frequency for the range of larger conductivity is now the upper resonance in the frequency splitting phenomenon. To allow frequency splitting to take place, the optimal load resistance is now much smaller, as shown in Fig. 2(d).

Since the system experiences both frequency-dependent eddy current losses and damping in the windings, the quantitative relationship between the medium losses and coils' internal resistances can be used to establish a criterion for the ‘switching point’ of the optimal working frequency. Figure 4 presents the simulation results for three extreme cases when (i)  $R_1 = 0$  and  $R_2 \neq 0$ , (ii)  $R_1 \neq 0$  and  $R_2 = 0$ , and (iii)  $R_1 = 0$  and  $R_2 = 0$ .

Interestingly, from Fig. 4, the non-zero receiver's resistance causes the switching point of the optimal frequency for maximum load power. Therefore, the switching point can be determined with respect to the receiver resistance by comparing the maximum output power at the uncoupled resonance and the upper one. Recall that  $f_u$  is the upper resonance frequency,  $P_0$  is the output power at  $\tilde{f}_0$ , and  $P_u$  is the output power at  $f_u$ . By solving the natural response of the two-coil system, the position of the upper and lower resonance can be approximated as<sup>13</sup>

$$f_{u,l} \approx \frac{\tilde{f}_0}{\Re \left[ \sqrt{1 \pm \frac{\mathcal{M}(\tilde{f}_0)}{L_0 + \Delta \mathcal{L}'(\tilde{f}_0)} - j \frac{\Delta \mathcal{L}''(\tilde{f}_0)}{L_0 + \Delta \mathcal{L}'(\tilde{f}_0)}} \right]}, \quad (6)$$

where  $f_{u,l}$  denotes the upper and lower resonance and  $\mathcal{M}(\tilde{f}_0)$  and  $\mathcal{L}(\tilde{f}_0)$  are the complex coefficients at  $\tilde{f}_0$ . By maximizing the output power subject to the value of the resistive load using (4), the maximum output powers at these two frequencies can be calculated as

$$P_{0(\max)} = \frac{\omega_0^2 |\mathcal{M}_0|^2 V_s^2}{2 \left[ A_0 R_2 + B_0 + \sqrt{A_0 \sqrt{A_0 R_2^2 + 2 B_0 R_2 + C_0}} \right]}, \quad (7)$$

$$P_{u(\max)} = \frac{\omega_0^2 |\mathcal{M}_0|^2 V_s^2}{2 \left[ A_u R_2 + B_u + \sqrt{A_u \sqrt{A_u R_2^2 + 2 B_u R_2 + C_u}} \right]}, \quad (8)$$

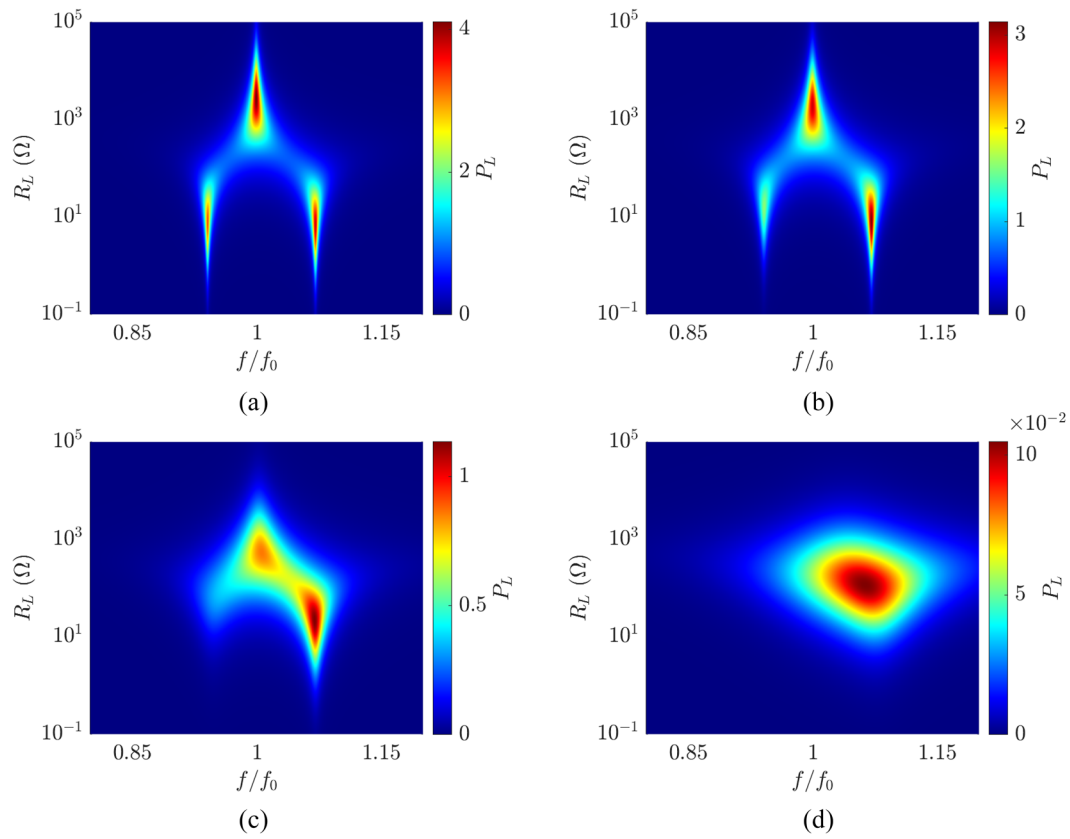


**FIG. 3.** Calculated color map of the output power  $P_L$  as a surface function of the normalized working frequency  $f$  and the load resistance  $R_L$ . The frequency is normalized by the resonance of the coils in the isolated case. The WPT system operates inside a medium with a conductivity of (a)  $\sigma = 0.01$ , (b)  $\sigma = 0.1$ , (c)  $\sigma = 1$ , and (d)  $\sigma = 10$  S/m.

where

$$\left\{ \begin{array}{l} A_k = (a_k^2 + b_k^2) \left( \frac{\omega_0 |\mathcal{M}_0|}{\omega_k |\mathcal{M}_k|} \right)^2, \\ B_k = [(a_k^2 + b_k^2)c_k + a_k e_k + b_k g_k] \left( \frac{\omega_0 |\mathcal{M}_0|}{\omega_k |\mathcal{M}_k|} \right)^2, \\ C_k = [(a_k^2 + b_k^2)(c_k^2 + d_k^2) + 2c_k(a_k e_k + b_k g_k) \\ + 2d_k(a_k g_k - b_k e_k) + e_k^2 + g_k^2] \left( \frac{\omega_0 |\mathcal{M}_0|}{\omega_k |\mathcal{M}_k|} \right)^2, \\ a_k = R_s + R_1 + \omega_k \mathcal{L}_{1,k}'', \\ b_k = \omega_k L_1 \left( 1 - \frac{\omega_0^2}{\omega_k^2} \right) + \omega_k \mathcal{L}_{1,k}', \\ c_k = \omega_k \mathcal{L}_{2,k}'', \\ d_k = \omega_k L_2 \left( 1 - \frac{\omega_0^2}{\omega_k^2} \right) + \omega_k \mathcal{L}_{2,k}', \\ e_k = \omega_k^2 (\mathcal{M}_k'^2 - \mathcal{M}_k''^2), \\ g_k = 2\omega_k^2 \mathcal{M}_k' \mathcal{M}_k'', \\ k = \{0, u\}. \end{array} \right. \quad (9)$$

The switching point occurs when  $P_u(\max) \geq P_0(\max)$ . It is equivalent to the inequality

$$(A_u - A_0)R_2 + B_u - B_0 \leq \sqrt{A_0} \sqrt{A_0 R_2^2 + 2B_0 R_2 + C_0} - \sqrt{A_u} \sqrt{A_u R_2^2 + 2B_u R_2 + C_u}. \quad (10)$$

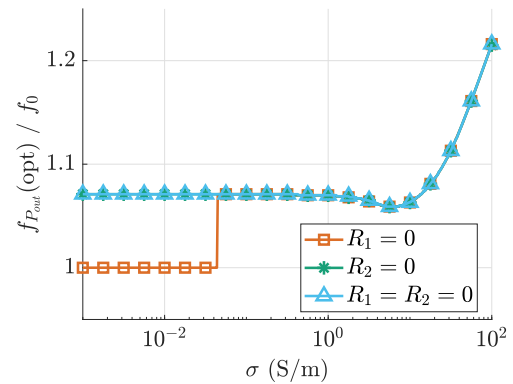


**FIG. 4.** Optimal frequency for the maximum output power at load for three extreme cases of the configuration:  $R_1 = 0 \Omega$ ,  $R_2 = 0 \Omega$ , and  $R_1 = R_2 = 0 \Omega$ .



Once the coefficients  $A_k$ ,  $B_k$ , and  $C_k$  are known, the inequality (10) is reducible to a quadratic inequality of variable  $R_2$ . The criteria for the switching point, therefore, can be formulated in terms of the internal resistance of the receiver,  $R_2$ .

The case study in the previous section is reinvestigated. By solving the inequality (10), the region for the optimal frequency for the maximum power at load can be determined. Figure 5 maps the comparison between output powers,  $P_0$  and  $P_u$ , vs the variation in the medium conductivity and the receiving coil resistance. The solid purple line refers to the equilibrium value when the strict equality occurs in (10), i.e.,  $P_0 = P_u$ . As shown in Fig. 5, when the damping of the secondary coil is very small, the optimal frequency is always the upper resonance regardless of the medium properties. Otherwise, once the medium conductivity is large enough, e.g.,  $\sigma \approx 8.1$  S/m for this configuration, the equilibrium line exhibits a vertical asymptote. It clearly demonstrates that the optimal working frequency in a highly conductive environment is the upper resonance due to the insurmountable loss by the medium at  $\tilde{f}_0$ .

The results in Fig. 5 provide guidance for practical coil designs inside common propagation media with the conductivity typically less than 5 S/m.<sup>17,18</sup> Since WPT systems often favor working at a single desired frequency set by regulating authorities, the original resonance of the coils in free space, the upper bound of the medium conductivity, where the system can function seamlessly, is generally computable on the basis of the receiver resistance and vice versa. The conductivity range of Fig. 5 corresponds to typical values of known earth materials and biomaterials. In addition, on the assumption that the system design allows flexibility in selecting the working frequency and the receiver resistance is estimated in advance, this switching point is significant for systems operating in time-varying natural environments, e.g., weather-dependent soils or seawater, and the human body. Otherwise, when the working frequency is fixed, employing electronically tunable coils would enable tracking the best performance for WPT systems in variable-conductivity media.

With this new circuit model for two coupled resonators in conductive environments, the mechanism for wireless power transfer in

these media has been analyzed. Unlike the free-space case, the working frequency selection requires more attention. In a similar study,<sup>20</sup> from the experimental results of the efficiency of the WPT system in seawater across a wide range of frequency, the authors concluded that the optimal working frequency should be higher than the resonant frequency in vacuum. Here, our simulation results show that the optimal frequency is not an arbitrary higher frequency but instead either the resonant frequency inside the medium [ $\tilde{f}_0$ , given by Eq. (5)] or the upper one due to the frequency splitting [ $f_u$ , given by Eq. (6)]. Surprisingly, the criterion for choosing the best working frequency is the quantitative relationship between the damping in the receiving coil and the eddy current losses. This criterion cannot be established if the complex frequency-dependent Kirchhoff's coefficients are not taken into account in the equivalent circuit model. The formula for frequency selection, which is reducible to a solvable quadratic inequality, can be used to construct a guidance map, based on the receiver's resistance and medium's electromagnetic property. It indeed offers insights to design and operate WPT systems in non-ideal environments.

This work was supported by EPSRC Grant No. EP/N010493/1 as a part of the SYMETA project ([www.symeta.co.uk](http://www.symeta.co.uk)). The authors wish to thank Professor Laszlo Solymar, Dr. Andrea Vallecchi, and fellow members of the Oxford Metamaterials Network (OxiMETA) for a number of fruitful discussions.

## AUTHOR DECLARATIONS

### Conflict of Interest

The authors have no conflicts to disclose.

## DATA AVAILABILITY

The data that support the findings of this study are available from the corresponding author upon reasonable request.

## REFERENCES

1. A. Kurs, A. Karalis, R. Moffatt, J. D. Joannopoulos, P. Fisher, and M. Soljačić, "Wireless power transfer via strongly coupled magnetic resonances," *Science* **317**, 83–86 (2007).
2. J. Garnica, R. A. Chinga, and J. Lin, "Wireless power transmission: From far field to near field," *Proc. IEEE* **101**, 1321–1331 (2013).
3. B. Wang, W. Yezazunis, and K. H. Teo, "Wireless power transfer: Metamaterials and array of coupled resonators," *Proc. IEEE* **101**, 1359–1368 (2013).
4. Z. Zhang, H. Pang, A. Georgiadis, and C. Cecati, "Wireless power transfer—An overview," *IEEE Trans. Ind. Electron.* **66**, 1044–1058 (2019).
5. H.-J. Kim, H. Hirayama, S. Kim, K. J. Han, R. Zhang, and J.-W. Choi, "Review of near-field wireless power and communication for biomedical applications," *IEEE Access* **5**, 21264–21285 (2017).
6. A. Vallecchi, E. Shamonina, and C. J. Stevens, "Wireless power transfer in the presence of a conducting interface: Analytical solution," *IET Microwaves Antenna Propag.* **13**, 725–731 (2019).
7. S. Chu, A. Vallecchi, C. J. Stevens, and E. Shamonina, "Fields and coupling between coils embedded in conductive environments," *EPJ Appl. Metamater.* **5**, 8 (2018).
8. S. C. Chu, "Near-fields in attenuating media," Ph.D. thesis, University of Oxford, 2019.

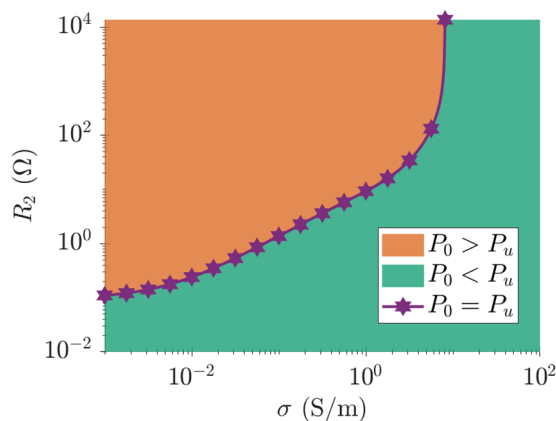


**FIG. 5.** Calculated color map guidance by using (10) for the optimal frequency selection as a function of the receiver resistance and the medium conductivity.

- <sup>9</sup>P. Liu, T. Gao, and Z. Mao, "Analysis of the mutual impedance of coils immersed in water," *Magnetochemistry* **7**, 113 (2021).
- <sup>10</sup>J. Kim, K. Kim, H. Kim, D. Kim, J. Park, and S. Ahn, "An efficient modeling for underwater wireless power transfer using  $z$ -parameters," *IEEE Trans. Electromagn. Compat.* **61**, 2006–2014 (2019).
- <sup>11</sup>K. Zhang, X. Zhang, Z. Zhu, Z. Yan, B. Song, and C. C. Mi, "A new coil structure to reduce eddy current loss of WPT systems for underwater vehicles," *IEEE Trans. Veh. Technol.* **68**, 245–253 (2019).
- <sup>12</sup>K. Zhang, Y. Ma, Z. Yan, Z. Di, B. Song, and A. P. Hu, "Eddy current loss and detuning effect of seawater on wireless power transfer," *IEEE Trans. Emerging Sel. Top. Power Electron.* **8**, 909–917 (2020).
- <sup>13</sup>S. Chu, M. S. Luloff, J. Yan, P. Petrov, C. J. Stevens, and E. Shamonina, "Magnetoinductive waves in attenuating media," *Sci. Rep.* **11**, 7679 (2021).
- <sup>14</sup>D. Zhou, L.-X. Pang, D.-W. Wang, C. Li, B.-B. Jin, and I. M. Reaney, "High permittivity and low loss microwave dielectrics suitable for 5G resonators and low temperature co-fired ceramic architecture," *J. Mater. Chem. C* **5**, 10094–10098 (2017).
- <sup>15</sup>W. Zhang and C. C. Mi, "Compensation topologies of high-power wireless power transfer systems," *IEEE Trans. Veh. Technol.* **65**, 4768–4778 (2016).
- <sup>16</sup>R. Tseng, B. V. Novak, S. Shevde, and K. A. Grajski, "Introduction to the alliance for wireless power loosely-coupled wireless power transfer system specification version 1.0," in *Proceedings of 2013 IEEE Wireless Power Transfer (WPT)* (IEEE, 2013), pp. 79–83.
- <sup>17</sup>G. J. Palacky, "Resistivity characteristics of geologic targets," in *Electromagnetic Methods in Applied Geophysics* (Society of Exploration Geophysicists, 1988), Chap. 3, pp. 52–129.
- <sup>18</sup>D. Miklavcic, N. Pavselj, and F. X. Hart, "Electric properties of tissues," in *Wiley Encyclopedia of Biomedical Engineering* (American Cancer Society, 2006).
- <sup>19</sup>X. S. Pu, T. H. Nguyen, D. C. Lee, K. B. Lee, and J. M. Kim, "Fault diagnosis of DC-link capacitors in three-phase AC/DC PWM converters by online estimation of equivalent series resistance," *IEEE Trans. Ind. Electron.* **60**, 4118–4127 (2012).
- <sup>20</sup>Z. Yan, Y. Zhang, T. Kan, F. Lu, K. Zhang, B. Song, and C. C. Mi, "Frequency optimization of a loosely coupled underwater wireless power transfer system considering eddy current loss," *IEEE Trans. Ind. Electron.* **66**, 3468–3476 (2018).